

Advances in FE explicit formulation for simulation of metalforming processes

J. Rojek^{a,*}, O.C. Zienkiewicz^b, E. Oñate^c, E. Postek^a

^aInstitute of Fundamental Technological Research, Polish Academy of Sciences, ul. Swietokryjska 21, PL-00049 Warsaw, Poland

^bUniversity of Wales, Swansea, UK

^cInternational Center for Numerical Methods in Engineering, Barcelona, Spain

Abstract

This paper presents some advances of finite element explicit formulation for simulation of metal forming processes. Because of their computational efficiency, finite element programs based on the explicit dynamic formulation proved to be a very attractive tool for the simulation of metal forming processes. The use of explicit programs in the sheet forming simulation is quite common, the possibilities of these codes in bulk forming simulation in our opinion are still not exploited sufficiently. In our paper, we will consider aspects of bulk forming simulation.

We will present new formulations and algorithms developed for bulk metal forming within the explicit formulation. An extension of a finite element code for the thermomechanical coupled analysis is discussed. A new thermomechanical constitutive model developed by the authors and implemented in the program is presented.

A new formulation based on the so-called split algorithm allows us to use linear triangular and tetrahedral elements in the analysis of large plastic deformations characteristic to forming processes. Linear triangles and tetrahedra have many advantages over quadrilateral and hexahedral elements. Linear triangles and tetrahedra based on the standard formulations exhibit volumetric locking and are not suitable for large plastic strain simulation. The new formulation allows to overcome this difficulty.

New formulations and algorithms have been implemented in the finite element code Stampack developed at the International Centre for Numerical Methods in Engineering in Barcelona. Numerical examples illustrate some of the possibilities of the finite element code developed and validate new algorithms. © 2001 Elsevier Science B.V. All rights reserved.

Keywords: Explicit formulation; Forming simulation; Split algorithm

1. Introduction

Finite element programs based on the explicit dynamic formulation proved to be a very attractive tool for the simulation of metalforming processes. The explicit time integration schemes deal with the system of discretized equations of motion in the following form:

$$\mathbf{M}\ddot{\mathbf{r}} + \mathbf{D}\dot{\mathbf{r}} = \mathbf{f} - \mathbf{p} \quad (1)$$

where \mathbf{M} and \mathbf{D} are the mass and damping matrices, \mathbf{r} the nodal displacement vector, and \mathbf{f} and \mathbf{p} the vectors of external and internal nodal forces, respectively. Employing Eq. (1) for the known configuration at time t_n , the solution for the next time instant $t_{n+1} = t_n + \Delta t$ is obtained. The effectiveness of the explicit formulation is based on the

use of a diagonal mass matrix. There are also disadvantages, the main one is the limitation of the time step due to the conditional stability. The numerical efficiency, however, and other advantages of explicit programs such as low memory requirements and easy treatment of contact conditions make this approach to dominate over implicit methods in industrial applications.

The computation times, however, in case of large industrial problems are still quite long. The implementation of a new triangular shell element as well as the use of techniques of parallel computations reduced simulation times considerably.

The use of explicit finite element programs in the analysis of sheet metal forming has become quite common, while the possibilities of this approach in the simulation of bulk forming seem not to be exploited sufficiently as yet. These problems require taking into account the thermal effects in the deformation process that can be achieved by the coupled thermomechanical analysis.

* Corresponding author.

E-mail address: jrojek@zmit1.ippt.gov.pl (J. Rojek).

2. Explicit thermomechanical analysis

2.1. Discretized equations of the coupled thermomechanical problem

Simulation of bulk forming processes usually requires taking into account the thermal effects and interaction of thermal and mechanical phenomena. The algorithm for a coupled thermomechanical analysis has been implemented in our explicit program, making it possible to analyse such forming processes.

In the solution of a thermomechanical problem, the solution of the mechanical problem (1) is coupled with the solution of the heat conduction problem governed by the following discretized equation:

$$\dot{\mathbf{C}}\dot{\mathbf{T}} + \mathbf{K}\mathbf{T} = \mathbf{Q} \quad (2)$$

where \mathbf{C} is the heat capacity matrix, \mathbf{K} the heat conductivity matrix, \mathbf{Q} the heat flux and sources vector, and \mathbf{T} the vector of nodal temperatures. Eqs. (1) and (2) are solved under adequate boundary conditions. Eq. (2) should be supplemented with thermal boundary conditions including heat convection and radiation, thermal effects on the tool surface should be taken into account as well. The forward Euler explicit time integration method has been implemented for the solution of Eq. (2) in the numerical algorithm for the thermomechanical analysis. This combined with the central difference time integration of Eq. (1) gives the following fully explicit scheme for a coupled problem:

$$\ddot{\mathbf{r}}_n = \mathbf{M}_D^{-1}(\mathbf{f}_n - \mathbf{p}_n - \mathbf{D}\dot{\mathbf{r}}_n), \quad \text{where } \mathbf{M}_D = \text{diag } \mathbf{M} \quad (3)$$

$$\dot{\mathbf{r}}_{n+1/2} = \dot{\mathbf{r}}_{n-1/2} + \ddot{\mathbf{r}}_n \Delta t \quad (4)$$

$$\mathbf{r}_{n+1} = \mathbf{r}_n + \dot{\mathbf{r}}_{n+1/2} \Delta t \quad (5)$$

$$\mathbf{T}_{n+1} = \mathbf{T}_n + \mathbf{C}_D^{-1}(\mathbf{Q}_n - \mathbf{K}\mathbf{T}_n) \Delta t, \quad \text{where } \mathbf{C}_D = \text{diag } \mathbf{C} \quad (6)$$

The new configuration \mathbf{r}_{n+1} is obtained from the explicit equations of motion with the temperatures assumed fixed,

and the new temperature \mathbf{T}_{n+1} is calculated at constant geometry. The results are exchanged at each step and coupling terms are calculated. Eqs. (1) and (2) for the thermomechanical problem are coupled by considering the following effects:

1. Heat generation by the plastic dissipation.
2. Contribution of the thermal expansion to the total material deformation.
3. Influence of the temperature on the yield stress of the material.

The rate of heat generation q due to the plastic dissipation (contributing to the vector \mathbf{Q}) can be calculated as

$$q = \chi \boldsymbol{\sigma} : \mathbf{d}^p \quad (7)$$

where $\boldsymbol{\sigma}$ is the Cauchy stress tensor, \mathbf{d}^p the rate of plastic deformation tensor, and χ the fraction of plastic work converted to heat. The method of accounting for the thermal effects in the constitutive model developed is presented in the next section.

2.2. Thermo-elastoplastic constitutive model

A new thermo-elastoplastic model has been developed and implemented in the explicit dynamic code Stampack. The model employs the concept of hyperelasticity. The main advantage of hyperelastic models compared to hypoelastic formulations is that there is no need for calculation of derivatives satisfying the criteria of objectivity and no need for integration of the constitutive equations [2,7].

Formulation of the constitutive model for the thermo-elastoplastic material is an extension of the elastoplastic model presented in [2] to the thermo-elastoplastic problems. In the description of large thermo-elastoplastic deformations, we assume the multiplicative decomposition (see Fig. 1) of the deformation gradient tensor \mathbf{F} into its elastic, thermal and plastic parts, \mathbf{F}^e , \mathbf{F}^θ and \mathbf{F}^p , respectively:

$$\mathbf{F} = \mathbf{F}^e \mathbf{F}^\theta \mathbf{F}^p \quad (8)$$

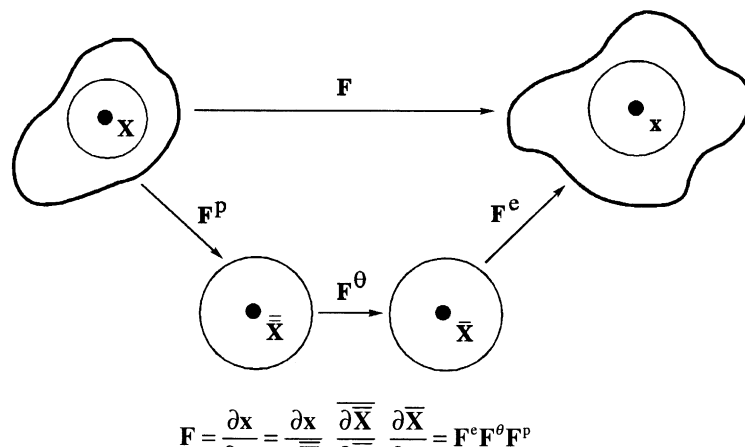


Fig. 1. Multiplicative decomposition of the deformation gradient tensor.

with

$$\det \mathbf{F}^p = 1 \quad (9)$$

$$\mathbf{F}^\theta = J^\theta \mathbf{I}, \text{ where } J^\theta = e^{3\alpha(T-T_0)} \quad (10)$$

The Almansi strain tensor \mathbf{e} can be expressed by means of the deformation gradient tensor \mathbf{F} as

$$\mathbf{e} = \frac{1}{2}(\mathbf{I} - \mathbf{F}^{-T}\mathbf{F}^{-1}) \quad (11)$$

Analogical to Eq. (11), we define the elastic Almansi tensor \mathbf{e}^e (in the spatial configuration) and the thermal Almansi tensor $\bar{\mathbf{e}}^\theta$ (in the intermediate configuration):

$$\mathbf{e}^e = \frac{1}{2}(\mathbf{I} - \mathbf{F}^{e-T}\mathbf{F}^{e-1}) \quad (12)$$

$$\bar{\mathbf{e}}^\theta = \frac{1}{2}(\mathbf{I} - \mathbf{F}^{\theta-T}\mathbf{F}^{\theta-1}) \quad (13)$$

After transforming the thermal Almansi tensor to the spatial configuration (the push-forward operation):

$$\mathbf{e}^\theta = \frac{1}{2}\mathbf{F}^{e-T}(\mathbf{I} - \mathbf{F}^{\theta-T}\mathbf{F}^{\theta-1})\mathbf{F}^{e-1} \quad (14)$$

we can introduce the following additive relation:

$$\mathbf{e} = \mathbf{e}^e + \mathbf{e}^\theta + \mathbf{e}^p \quad (15)$$

defining the plastic Almansi tensor \mathbf{e}^p . Applying the Lie derivative L_v to all the components of the Almansi tensor in Eq. (15), we obtain the additive decomposition of the deformation rate tensor

$$\mathbf{d} = \mathbf{d}^e + \mathbf{d}^\theta + \mathbf{d}^p \quad (16)$$

The stress response is characterised by means of the elastic free energy function of the form

$$\psi^e = \frac{1}{2}\lambda \operatorname{tr}(\mathbf{e}^e) + \mu(\mathbf{e}^e : \mathbf{e}^e) \quad (17)$$

where λ and μ are the Lamé constants. With this form of the elastic potential the constitutive relation obtained for the Cauchy stresses is following:

$$\sigma = \frac{\partial \psi(\mathbf{e}^e)}{\partial \mathbf{e}^e} = \lambda \operatorname{tr} \mathbf{e}^e + 2\mu \mathbf{e}^e \quad (18)$$

The stresses are calculated in a two-step algorithm, the first step is the elastic predictor, and the second one the plastic corrector employing the radial return. For the plastic deformation, the associated flow rule is assumed:

$$\mathbf{d}^p = L_v(\mathbf{e}^p) = \dot{\lambda} \frac{\partial f}{\partial \sigma} \quad (19)$$

with the Von Mises yield condition:

$$f = \sqrt{\frac{3}{2}\tau : \tau} - \sigma_Y(\varepsilon^p, T) \leq 0 \quad (20)$$

that accounts for the isotropic hardening and thermal softening:

$$\sigma_Y = [\sigma_0 + (\sigma_\infty - \sigma_0)(1 - e^{-\delta\varepsilon^p}) + He^p][1 - H_\theta(T - T_0)] \quad (21)$$

where τ is the deviatoric Cauchy stress, tensor σ_0 and σ_∞ the initial and the final yield stresses, δ the saturation constant, H the hardening modulus and H_θ the thermal softening modulus.

The form of the elastic potential (17) is based on the assumption that the elastic part of the strains \mathbf{e}_e is small, which is fully justified for metals. It is assumed for the reasons of simplicity and efficiency. Some authors starting from the same basic assumption expressed by Eq. (8), cf. [8–10], have developed more general models, considering the possibility of large elastic deformations. Our formulation is simpler in implementation and no loss of accuracy in the considered class of problems is expected. A good behaviour of this model in the problems of metal forming without accounting for thermal effects has been confirmed earlier, cf. [2,3].

2.3. Finite element implementation

The developed thermo-elastoplastic model has been implemented in the program Stampack with a 4-node plane strain and axisymmetric element and with an 8-node hexahedral element for three-dimensional analysis. In both the elements, the mixed formulation (with constant pressure) has been used to avoid element locking. These elements are typically used in all the dynamic codes in the problems involving large plastic deformations. Linear triangles and tetrahedra experience volumetric locking in the problems with incompressible or nearly incompressible deformations like those in bulk forming processes. This introduces serious limitations on meshing a complex geometry. Until now meshing programs work better with triangular and tetrahedral elements. To overcome this problem, we have adapted the so-called split allowing us to use linear triangles and tetrahedra [13]. The formulation of the split algorithm is presented below.

3. Linear triangles and tetrahedra within the split algorithm

3.1. Finite element formulations for incompressible problems

Finite elements based on the standard displacement formulation are vulnerable to volumetric locking in the analysis of problems with incompressible deformations. This poses serious problems in the simulation of elasto-plastic cases. Introduction of a small compressibility does not yield a solution, elements that do not perform well in an incompressible state do not give good results in nearly incompressible state either.

Different methods have been developed to overcome this problem. Some of them employ the mixed finite element formulation in which we split the stresses σ into the deviatoric part τ and pressure p :

$$\sigma = \tau + \mathbf{I}p \quad (22)$$

Then using independent interpolations for displacements $\mathbf{r} = \mathbf{N}_d \bar{\mathbf{r}}$ and pressure $p = \mathbf{N}_p \bar{p}$ (\mathbf{N}_d and \mathbf{N}_p are shape functions, $\bar{\mathbf{r}}$ and \bar{p} the nodal values of displacements and pressure), we obtain the following set of mixed equations cf. [9,10]:

$$\begin{bmatrix} \mathbf{K} & \mathbf{Q} \\ \mathbf{Q}^T & \mathbf{G} \end{bmatrix} \begin{bmatrix} \bar{\mathbf{r}} \\ \bar{p} \end{bmatrix} = \begin{bmatrix} \mathbf{f}_d \\ \mathbf{f}_p \end{bmatrix} \quad (23)$$

In compressible case $\mathbf{G} \neq \mathbf{0}$ and \bar{p} can be eliminated:

$$(\mathbf{K} - \mathbf{Q}\mathbf{G}^{-1}\mathbf{Q}^T)\bar{\mathbf{r}} = \mathbf{f}_d - \mathbf{Q}\mathbf{G}^{-1}\mathbf{f}_p \quad (24)$$

If pressure is discontinuous between elements, \bar{p} can be eliminated at the element level.

In incompressible state $\mathbf{G} = \mathbf{0}$, the following equation for pressure can be obtained:

$$(\mathbf{Q}^T\mathbf{K}^{-1}\mathbf{Q})\bar{p} = \mathbf{Q}^T\mathbf{K}^{-1}\mathbf{f}_d - \mathbf{f}_p \quad (25)$$

Not all combinations of displacement and pressure interpolations (\mathbf{N}_d and \mathbf{N}_p) are allowed since some of them render the coefficient matrix $\mathbf{Q}^T\mathbf{K}^{-1}\mathbf{Q}$ singular. Then the effect of volumetric locking appears. This happens in case of linear triangles and tetrahedra with equal order interpolation of displacement and pressure. A mathematical theory has been established for mixed elements [4]. This theory is fundamental of the Babuska–Brezzi stability condition [4].

Special techniques have been developed to avoid locking in elements not satisfying Babuska–Brezzi condition. One of the methods is the so-called selective integration in which the volumetric components are integrated in some of the Gauss points only. For economy, selective integration is often replaced by the so-called reduced integration. Hughes [5] developed a stabilization procedure consisting in adding of the equilibrium equation suitably weighted by the shape functions to the mass conservation equation. Bonet [1] derived for explicit dynamic applications a linear tetrahedron free of volumetric locking using the idea of averaging nodal pressure.

Our stabilising procedure is based on the split algorithms developed in fluid mechanics [11,12]. Appropriate splitting of the equations of motion allows equal order interpolation to be used in incompressible flows. Adapting this method to solid mechanics and explicit dynamic program, we have obtained 3-node triangular and 4-node tetrahedral elements that can be used in nearly incompressible problems of bulk metal forming. The basic equations of the split algorithm are presented below, more details has been given by Zienkiewicz et al. [13].

3.2. The split algorithm

The split operator will be applied to the Stokes equations for nearly incompressible flow:

$$\rho_0 \frac{\partial v_i}{\partial t} = \frac{\partial \tau_{ij}}{\partial x_j} - \frac{\partial p}{\partial x_i} + g_i \quad (26)$$

$$\frac{1}{c^2} \frac{\partial p}{\partial t} = -\rho_0 \frac{\partial v_i}{\partial x_i} \quad (27)$$

where ρ_0 is the density, v_i the velocity in the i th direction, τ_{ij} the deviatoric stress component, p the pressure (or mean stress), g_i the i th component of body force, and c the speed of sound given by the relation $c = \sqrt{K/\rho_0}$, K being the bulk modulus. After discretization the Stokes equation can be written in the following form [9,10]:

$$\begin{bmatrix} \mathbf{M} & \mathbf{0} \\ \mathbf{0} & \tilde{\mathbf{M}} \end{bmatrix} \frac{d}{dt} \begin{bmatrix} \bar{\mathbf{v}} \\ \bar{p} \end{bmatrix} + \begin{bmatrix} \mathbf{K} & \mathbf{Q} \\ \mathbf{Q}^T & \mathbf{0} \end{bmatrix} \begin{bmatrix} \bar{\mathbf{v}} \\ \bar{p} \end{bmatrix} = \begin{bmatrix} \mathbf{f}_d \\ \mathbf{f}_p \end{bmatrix} \quad (28)$$

In the above, the standard finite element notation is used [9,10].

A clear analogy between Eqs. (23) and (28) can be noted here. Similarly like in case of Eq. (23) for incompressible problem, the zero diagonal term in the second matrix of Eq. (28) leads to volumetric locking. The splitting algorithm removes this problem.

In the described algorithm, Eq. (28) is split into parts in such a way, however, that the sum of the parts gives the original equation (28). Let us rewrite Eq. (28) in the following form:

$$\mathbf{M}\dot{\bar{\mathbf{v}}} = \mathbf{f}_v - \mathbf{K}\bar{\mathbf{v}} - \mathbf{Q}\bar{p} \quad (29)$$

$$\tilde{\mathbf{M}}\bar{p} = -\mathbf{Q}^T\bar{\mathbf{v}} \quad (30)$$

In the explicit split algorithm, the time integration schemes (3) and (4) is modified in the following way:

1. Approximate velocity determination (from the momentum conservation equation (29) omitting pressure terms):

$$\bar{\mathbf{v}}^* = \bar{\mathbf{v}}_{n-1/2} + \Delta t \mathbf{M}^{-1} (\mathbf{f}_v - \mathbf{K}\bar{\mathbf{v}}_{n-1/2}) \quad (31)$$

2. The pressure evaluation (from the mass conservation equation (30)):

$$\bar{p}_{n+1} = \bar{p}_n - \Delta t \tilde{\mathbf{M}}^{-1} (\mathbf{Q}\bar{\mathbf{v}}^* - \Delta t \mathbf{H}\bar{p}_n) \quad (32)$$

where \mathbf{H} is the standard discretization of the Laplacian operator.

3. The velocity correction (from the momentum conservation equation (29) taking into account step 1):

$$\bar{\mathbf{v}}_{n+1/2} = \bar{\mathbf{v}}^* - \Delta t \mathbf{M}^{-1} \mathbf{Q}\bar{p}_n \quad (33)$$

The described explicit split algorithm implemented for linear triangles and tetrahedra has been successfully applied to thermomechanical analysis. Test examples of bulk forming are included in the paper.

3.3. Why is the Babuska–Brezzi condition circumvented?

When steady state conditions are reached, we have

$$\bar{\mathbf{v}}_{n+1/2} = \bar{\mathbf{v}}_{n-1/2} = \bar{\mathbf{v}}, \quad \bar{p}_{n+1} = \bar{p}_n = \bar{p} \quad (34)$$

After substituting relations (34) into Eqs. (30)–(32) and eliminating $\bar{\mathbf{v}}^*$ we obtain the system of the following form

$$\begin{bmatrix} \mathbf{K} & \mathbf{Q} \\ \mathbf{Q}^T & \Delta t(\mathbf{H} - \mathbf{QM}\mathbf{Q}) \end{bmatrix} \begin{bmatrix} \bar{\mathbf{v}} \\ \bar{p} \end{bmatrix} = \begin{bmatrix} \mathbf{f}_d \\ \mathbf{0} \end{bmatrix} \quad (35)$$

The term on the diagonal involving the variable \bar{p} is no longer zero. This illustrates the stabilizing effect of the split

algorithm. The proof that the equation set (35) is well conditioned can be found in [11].

4. Numerical examples

4.1. Impact of a cylindrical bar

The example studied here is that of an impact with a rigid surface of a cylindrical rod moving with a high speed. This problem is frequently studied by explicit dynamics codes. This example is aimed to show the correctness of the split formulation with linear triangles and tetrahedra that will be used for metal forming simulation.

The material properties for an elasto-plastic model are: modulus of elasticity, 117 GPa; Poisson ratio, $\nu = 0.35$, initial uniaxial yield stress, $\sigma_0 = 0.4$ GPa; and hardening modulus, $H = 0.1$ GPa. The initial length of the bar is 32.4 mm and the initial radius is 3.2 mm. A solution is obtained for an initial velocity of 227 m/s. The interval of 80 μ s has been analysed which allows the body to reach a steady state. The final deformed shapes obtained using different formulations are shown in Fig. 2. The results of the mixed formulation with Q1/P0 8-node elements are shown in Fig. 2a. The cases (b) and (c) show wrong solutions with the effect of locking. The solutions (d) and (e) are obtained using the split algorithm and linear triangles and tetrahedra. As it can be noted, these solutions are practically identical with the solution (a). The effect of locking has been eliminated.

4.2. Upsetting of a cylindrical billet

This example was used to verify the new thermoelastoplastic constitutive model and to test the algorithm of thermomechanical analysis implemented in the program Stampack. A cylindrical billet, 30 mm high and with a radius

of 10 mm, is compressed along its axis between two rigid and rough plates. All the surfaces are assumed to be fully insulated. The problem has been defined originally by Lippmann [6] and was analysed in [14]. The analysis was carried out to 60% upsetting. The mechanical and thermal properties were the following: Young's modulus: $E = 2 \times 10^5$ MPa, Poisson's coefficient: $\nu = 0.3$, density: $\rho = 7830$ kg/m³, yield stress: $\sigma_0 = \sigma_\infty = 700$ MPa, hardening modulus: $H = 300$ MPa, thermal softening modulus: $H_\theta = 0.002$ °C⁻¹, specific heat: $c = 586$ J/kg °C, conductivity: $k = 52$ W/m °C. The material properties were basically the same as those used in [14] except that thermal softening was considered and rate-independent plasticity was assumed in our models. The final deformation was obtained in 0.1 s.

Both two- and three-dimensional simulation were carried out. In 2D two models were studied, a half of the billet was discretized with 144 quadrilateral and 288 triangular axis-symmetric elements, the latter case was analysed using the split algorithm. The results of the analysis for both cases are shown in Fig. 3. Fig. 3 shows the final deformed shapes with the temperature distribution. Similar results have been obtained with quadrilateral and triangular mesh. The results coincide with the results obtained with the implicit ABAQUS [14]. Three-dimensional solution obtained using tetrahedra with the split algorithm is given in Fig. 4. The results of this example confirm the accuracy and correctness of the thermomechanical model and algorithm implemented in our explicit dynamic program. This example shows a good behaviour of linear triangles and tetrahedra within the split algorithm in the thermomechanical coupled analysis.

4.3. Sidepressing of a cylinder

A cylinder 100 mm long with a radius of 100 mm is subjected to sidepressing between two plane dies. It is

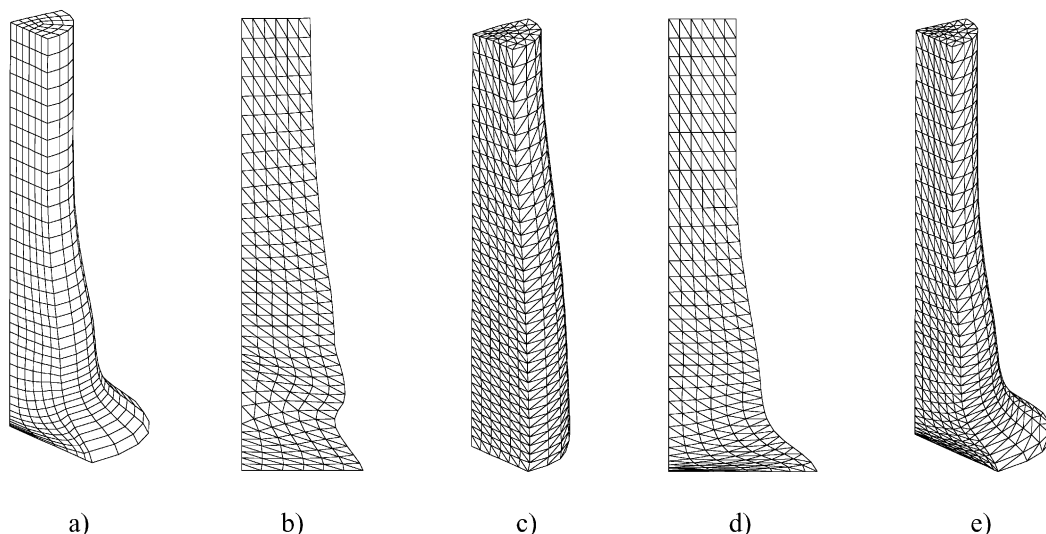


Fig. 2. Deformed shapes of the bar after impact. Different solutions: (a) Q1/P0 hexahedral elements, mixed algorithm; (b) linear triangles, displacement formulation (locking); (c) tetrahedral elements, displacement formulation (locking); (d) linear triangles, split algorithm; (e) tetrahedral elements, split algorithm.

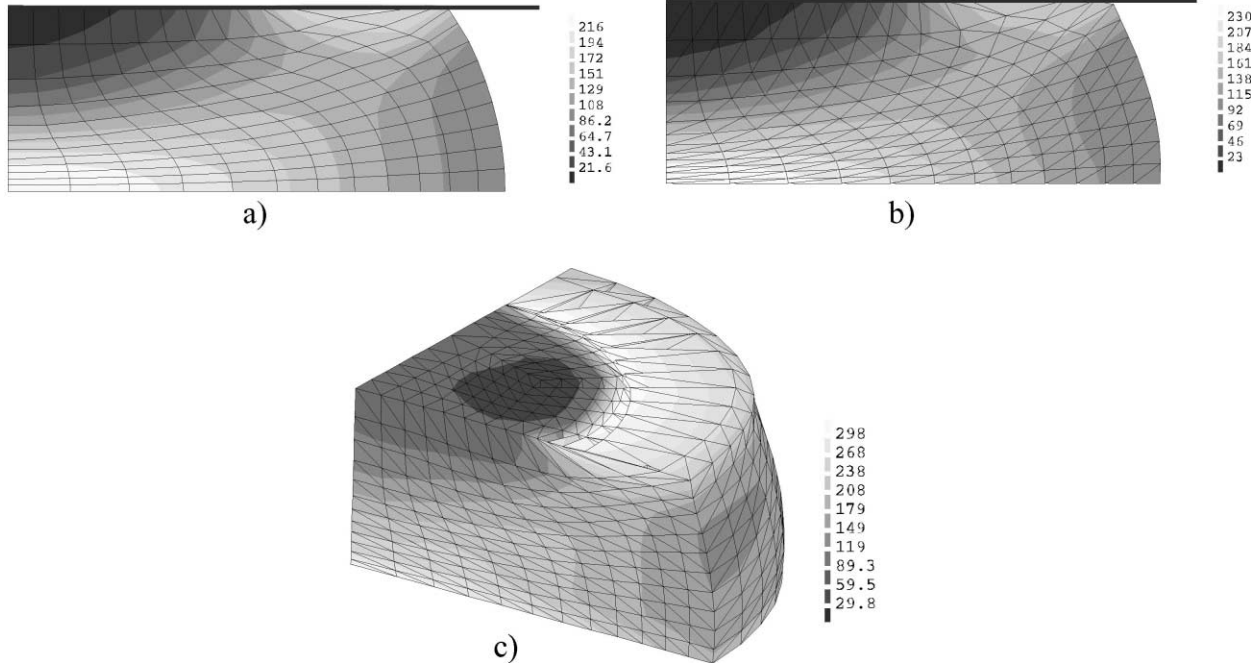


Fig. 3. Upsetting of a cylindrical billet — deformed shape at 60% upsetting with the temperature distribution: (a) quadrilaterals, mixed formulation; (b) triangles; (c) tetrahedra, split algorithm.

compressed to 100 mm. The material properties are the following: $E = 217 \text{ GPa}$, $v = 0.3$, $\rho = 7830 \text{ kg/m}^3$, $\sigma_0 = 170 \text{ MPa}$, $H = 30 \text{ MPa}$, $c = 586 \text{ J/kg }^\circ\text{C}$, $k = 52 \text{ W/m }^\circ\text{C}$, friction coefficient = 0.2. The die velocity is assumed to

be 2 m/s. A quarter of a cylinder was discretized. Initial set-up is shown in Fig. 4a. This example demonstrates the agreement between the explicit dynamic solution with STAMPACK (Fig. 4c) and quasistatic implicit solution with

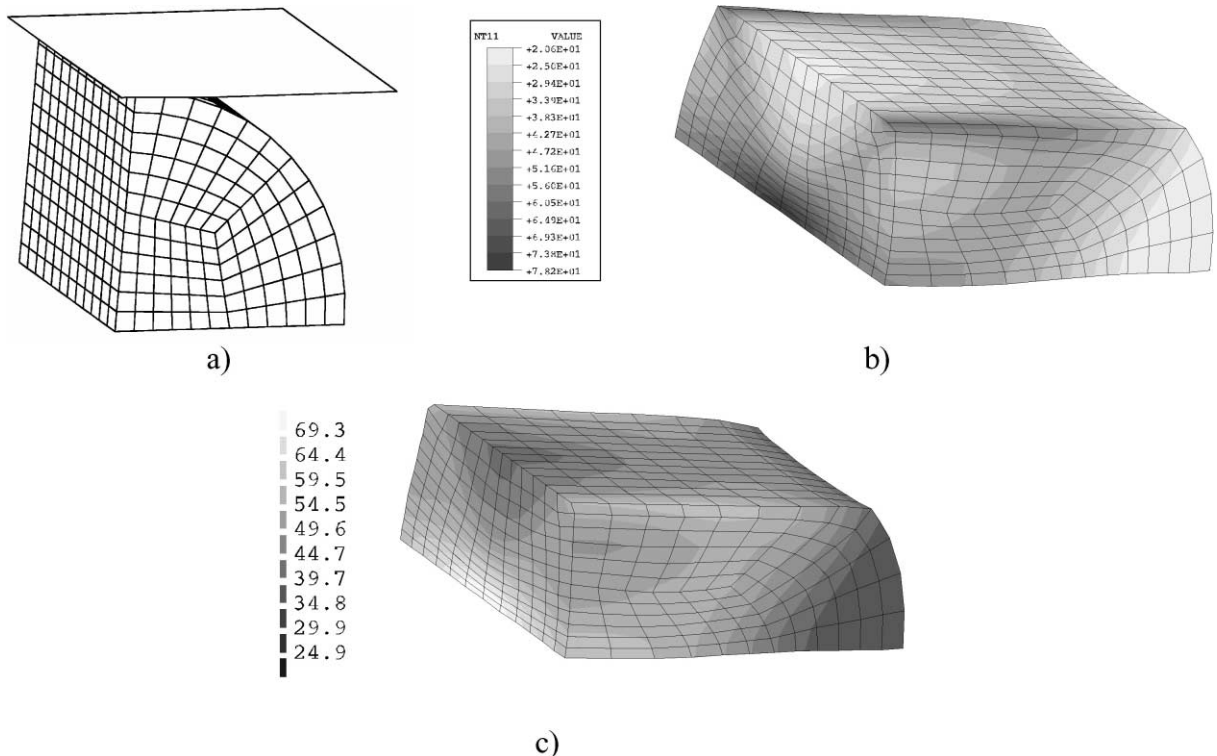


Fig. 4. Sidepressing of a cylinder: (a) initial mesh; (b) temperature distribution — implicit solution (ABAQUS); (c) temperature distribution — explicit solution (STAMPACK).

ABAQUS (Fig. 4b). Far more efficient is the explicit solution, it took 18 min CPU on Pentium II 350 MHz, while the implicit analysis took about 8 h CPU on Cray J916. Unfortunately, we do not have the comparisons for the same platform, but this demonstrates the computational efficiency of the explicit solution in comparison with the implicit one.

5. Concluding remarks

The explicit thermomechanical algorithm and the split algorithm, implemented in the finite element explicit program STAMPACK have given good results for benchmark examples of bulk forming. A good agreement between implicit quasistatic and explicit dynamic results have been observed, at the same time in 3D analysis a considerable advantage of explicit program has been seen. This allows us to see good perspectives in the use of our explicit code in the simulation of industrial problems of bulk forming. For this purpose, further development of the software, including adaptive remeshing, is planned.

Acknowledgements

The first and fourth author gratefully acknowledge the funding from the Polish Committee for Scientific Research under Grant No. 8 T11F 015 12.

References

- [1] J. Bonet, A.J. Burton, A simple average nodal pressure tetrahedral element for incompressible and nearly incompressible dynamic explicit applications, *Commun. Num. Meth. Eng.* 14 (1998) 437–449.
- [2] C.G. Garino, J. Oliver, Use of a large strain elastoplastic model for simulation of metal forming processes, in: J.L. Chenot, R. Wood, O.C. Zienkiewicz (Eds.), *NUMIFORM '92*, Balkema, 1992.
- [3] C.G. Garino, J. Rojek, E. Oñate, Simulation of sheet metal stamping processes using a solid finite strain model, in: L.A. Godoy, S.R. Idelsohn, P.A.A. Laura, D.T. Mook (Eds.), *Applied Mechanics in the Americas*, Vol. 1, Santa Fe, Argentina, 1995, pp. 97–102.
- [4] T.J.R. Hughes, *The Finite Element Method. Linear Static and Dynamic Finite Element Analysis*, Prentice-Hall, Englewood Cliffs, NJ 1987.
- [5] T.J.R. Hughes, L.P. Franca, M. Balestre, A new finite element formulation for computational fluid dynamics. V. Circumventing the Babuska–Brezzi condition: a stable Petrov–Galerkin formulation for the Stokes problem accommodating equal-order interpolations, *Comput. Meth. Appl. Mech. Eng.* 59 (1986).
- [6] H. Lippmann, *Metal Forming Plasticity*, Springer, Berlin, 1979.
- [7] J.C. Simo, M. Ortiz, A unified approach to finite deformation elastoplastic analysis based on the use of hyperelastic constitutive relations, *Comput. Meth. Appl. Mech. Eng.* 49 (1985).
- [8] P. Wriggers, C. Miehe, M. Kleiber, J.C. Simo, On the coupled thermomechanical treatment of necking problems via finite element methods, *Int. J. Num. Meth. Eng.* 33 (1992) 869–883.
- [9] O.C. Zienkiewicz, R.L. Taylor, *The Finite Element Method*, 4th Edition, Vol. 1, McGraw-Hill, London, 1989.
- [10] O.C. Zienkiewicz, R.L. Taylor, *The Finite Element Method*, 4th Edition, Vol. 2, McGraw-Hill, London, 1991.
- [11] O.C. Zienkiewicz, R. Codina, A general algorithm for compressible and incompressible flow — Part I. The split, characteristic-based scheme, *Int. J. Num. Meth. Fluids* 20 (1995) 869–885.
- [12] O.C. Zienkiewicz, K. Morgan, B.V.K. Satya Sai, R. Codina, M. Vasquez, A general algorithm for compressible and incompressible flow — Part II. Tests on the explicit form, *Int. J. Num. Meth. Fluids* 20 (1995) 887–913.
- [13] O.C. Zienkiewicz, J. Rojek, R.L. Taylor, M. Pastor, Triangles and tetrahedra in explicit dynamic codes for solids, *Int. J. Num. Meth. Eng.* 43 (1998) 565–583.
- [14] ABAQUS, Example Manual, Version 5.6, Hibbit, Karlsson & Sorensen, Inc., 1996.